Search for differences between radio-loud and radio-quiet gamma-ray pulsar populations with Fermi-LAT data

E. V. Sokolova and G. I. Rubtsov

Institute for Nuclear Research of the Russian Academy of Sciences, Moscow 117312, Russia

Observations by Fermi LAT enabled us to explore the population of non-recycled gamma-ray pulsars with the set of 89 objects. It was recently noted that there are apparent differences in properties of radio-quiet and radio-loud subsets. In particular, average observed radio-loud pulsar is younger than radio-quiet one and is located at smaller galactic latitude. Even so, the analysis based on the full list of pulsars may suffer from selection effects. Namely, most of radio-loud pulsars are first discovered in the radio-band, while radio-quiet ones are found using the gamma-ray data. In this work we perform a blind search for gamma-ray pulsars using the Fermi LAT data alone using all point sources from 3FGL catalog as the candidates. Unlike preceding blind search, the present catalog is constructed with novel semi-coherent method and covers the full range of characteristic ages down to 1 kyr. The search resulted in the catalog of 40 non-recycled pulsars, 26 of which are radio-quiet. There are no statistically significant differences in age and galactic latitude distributions for the radio-loud and radio-quiet pulsars, while the rotation period distributions are marginally different with 2.4σ pre-trial statistical significance. The fraction of radio-quiet pulsars is estimated as $\epsilon_{RQ} = 63 \pm 8\%$. The results are in agreement with the predictions of the outer magnitosphere models, while the Polar cap models are disfavored.

I. INTRODUCTION

The number of known gamma-ray pulsars grows rapidly since the Fermi Large Area Telescope (LAT) started taking data in August 2008. At present 160 gamma-ray pulsars are identified, including 89 non-recycled pulsars. The latter include 53 radio-loud pulsars and 36 radio-quiet ones, see [1, 2] for review. With the only exception of Geminga [3, 4], detection of the radio-quiet pulsars became possible only with the sensitivity of Fermi LAT. High-performance numerical methods were designed and implemented, including time-differencing technique [5, 6] and the semi-coherent method [7–9].

With the statistics in hands one may raise questions on the model of the gamma-ray emission and corresponding mechanism of the radio-quietness. Two general classes of the pulsar gamma-ray emission models are discussed. First class includes the so-called Polar cap (PC) models [10]. In these models gamma-rays are produced by electrons and positrons accelerated in the polar cap region near the surface of the neutron star. In the PC models the gamma-ray and radio beams are generally co-aligned. The latter is considered narrower that the former and therefore some of the pulsars are observed as radio-quiet [11]. Moreover, in the PC models the fraction of the radio-quiet pulsars depends on the pulsar's age [12]. In the second class of models the gamma-ray emission is produced in the outer magnetosphere (OM) of the pulsar [13, 14]. In the OM models the radio-quietness finds geometrical description as the gamma-ray and radio-beams orientations are naturally diverse.

It was noted that the observed fraction of the radio-quiet objects is relatively small for young pulsars [15]. This observation may be interpreted in terms of evolution of the radio-beam solid angle [15, 16]. Alternatively this may be an effect of the observational selection bias [1]. While radio-quiet pulsars are discovered in a blind search with gamma-ray data, there are multiple ways to find radio-loud pulsars. The latter may be found either in radio surveys or with follow-up observations of gamma-ray sources. In most cases the gamma-ray pulsations of radio-loud pulsars are found with ephemerides from radio observations. Nevertheless there are pulsars with pulsed radio-emission detected following the gamma-ray pulsations.

In this *Paper* we construct a bias-free catalog of the gamma-ray selected pulsars by performing a blind search for gamma-ray pulsars using the Fermi LAT data alone. The search is more extensive with respect to the preceding blind search [17]. With the novel efficient semi-coherent method a complete range of characteristic ages starting from 1 kyr is covered. No radio or optical observation data are used.

The paper is organized as follows. Fermi LAT data selection and preparation procedures are explained in Section II. The implementation details of the semi-coherent method are given in Section III. The catalog of the gamma-ray selected pulsars, comparison of radio-quiet and radio-loud gamma-ray pulsars populations and comparison of the results to the predictions of the pulsar emission models are presented in Section IV.

II. DATA

The paper is based on publicly available weekly all-sky Fermi LAT data for the time period from August 4, 2008 till March 3, 2015 (Mission elapsed time from 239557418 to 447055673 s) [18, 19]. We select SOURCE class events from Reprocessed Pass 7 data set with energies from 100

MeV to 300 GeV. The standard quality cuts are applied using *Fermi Science Tools v9r32p5* package. These include 100° and 52° upper constraints for zenith angle and satellite rocking angle.

We search for pulsations using the location of each of 3008 point sources from the Fermi LAT 4-year Point Source Catalog (3FGL) [20]. The requirement of blindness to everything except gamma-ray emission binds us to the coordinates from the 3FGL catalog. Although the precision of the gamma-ray source positioning is one of the factors limiting sensitivity of the scan [7] we did not scan over the sky location due to computational complexity.

A model of the 8° radius circle sky patch is constructed for each of the candidates. The model includes galactic and isotropic diffuse emission components and all 3FGL sources within 8° from the position of interest. We optimize the parameters of the model with *gtlike* tool and then using *gtsrcprob* assign each photon a weight - probability to originate from the given pulsar candidate. For computational efficiency we keep 40000 event with the highest weights for each source. Finally, the photon arrival times are converted to barycentric frame using *gtbary* tool.

III.   METHOD

The search for pulsations is performed with the semi-coherent method proposed by Pletsch et al. [7] We scan over pulsar's frequency f and spin-down rate $\dot{f}$ using the list of barycentric photon arrival times t_a and corresponding weights w_a. First, the arrival times are corrected to compensate for frequency evolution

$$\tilde{t} = t + \frac{\gamma}{2}(t - t_0)^2 \,, \tag{1}$$

where $\gamma = \dot{f}/f$ and $t_0 = 286416002$ (MJD 55225) is a reference epoch. The spectral density P_m is obtained with a Fourier transform of the time differences

$$P_m = \text{Re} \sum_{a,b=1} \Pi(\Delta t_{ab}/2T) w_a w_b e^{-2\pi i f_m \Delta t_{ab}}, \tag{2}$$

where $\Delta t_{ab} = t_b - t_a$, $f_m = m/T$, $T = 2^{19}$ and $\Pi(x)$ is the rectangular function which takes the value of 1 for $-0.5 < x < 0.5$ and 0 otherwise. Technically we consider only positive time differences and bin the time interval $(0, T)$ into $N = 2^{26}$ bins. With the cycle over all event pairs one calculates the sum of product of weights $w_a w_b$ in each bin. This prepares an input for fast Fourier transform performed with the open source library *fftw* [21].

The Nyquist frequency is $N/2T = 64\,\text{Hz}$. We scan over the parameter γ from 0 to -1.6×10^{-11} with a step equal to -1×10^{-15}. The range corresponds to the pulsar characteristic age greater than $1\,\text{kyr}$.

The values of f and $\dot{f}$ corresponding to the highest P_m are used as a starting point for the final coherent
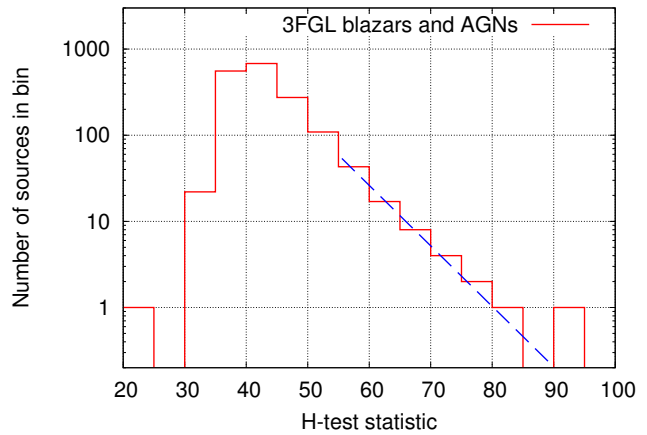

FIG. 1. The distribution of H-test statistic for 3FGL indentified blazars

scan. The latter is performed with maximization of the weighed H-test statistic [22] defined as follows:

$$H = \max_{1 \leq L \leq 20} \left[\sum_{l=1}^{L} \mid \alpha_l \mid^2 - 4(L-1) \right] \,, \tag{3}$$

where α_l is a Fourier amplitude of the l-th harmonic

$$\alpha_l = \frac{1}{\varkappa} \sum_a w_a \exp^{-2\pi i l f \tilde{t}_a} \,,$$

$$\varkappa^2 = \frac{1}{2} \sum_a w_a^2 \,.$$

We take into account that a combination of the pulsar's frequency and an inverse Fermi orbital period T_{LAT} may be found at the semi-coherent stage. Therefore, the H-test is repeated three times starting from f, $f + 1/T_{LAT}$ and $f - 1/T_{LAT}$.

In this work an extensive scanning is performed and therefore a theoretical distribution of H-test statistic for the null hypothesis of non-pulsating object may not be used directly. We estimate the H distribution using the results of the scan for the 1720 3FGL objects identified as blazars, see Fig. 1. We extrapolate the tail of the distribution with the exponential function and require that the probability to have a single false candidate in the whole scan is less than 5%. Thus we arrive to the threshold value $H_{th} = 98$. Unlike the rest of the work here we used identification information to select blazars from all the sources. We note that this does not affect detection uniformity since the same H_{th} is then used for all sources. Moreover, the procedure stays conservative in case of pulsar contamination in the blazars sample. In this case the H_{th} would be overestimated and the probability of the false candidate appearance even less than required.
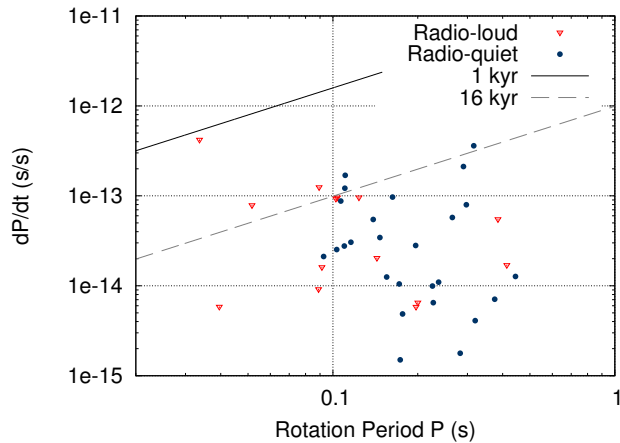
FIG. 2. $P - \dot{P}$ plot for 40 pulsars found with a blind search in the present *Paper*. $P = \frac{1}{f}$ is a rotation period. The lines show maximum characteristics ages for present and previous blind searches.

FIG. 4. Distributions of the rotation period P for radio-loud and radio-quiet pulsars. The two distrubutions are compatible with KS probability 1.5%.
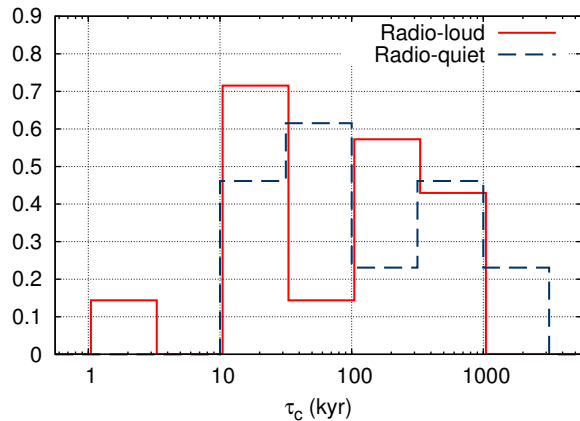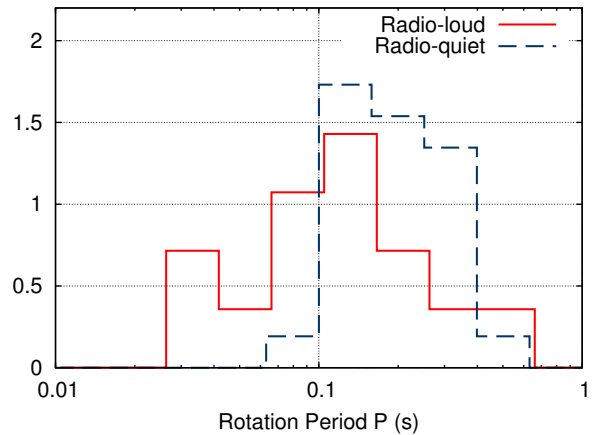

FIG. 3. Distributions of characteristic age $\tau_c = -\frac{f}{2\dot{f}}$ for radio-loud and radio-quiet pulsars. The two distrubutions are compatible with KS probability 43%.

FIG. 5. Distributions of $\dot{P}$ for radio-loud and radio-quiet pulsars. The two distrubutions are compatible with KS probability 85%.

IV. RESULTS

There are 40 pulsating sources found in a blind search, see Table II for the complete catalog. All the sources found in these *Paper* were known previously as the gamma-ray pulsars. These include 26 radio-quiet and 14 radio-loud pulsars. We note that all 25 pulsars from the previous blind search [17] are also found here.

We compare the distributions of the observed parameters for the radio-loud and radio-quiet pulsars with the Kolmogorov-Smirnov test and summarize the results in Table I and Figures 2-7. There are no statistically significant differences in characteristic age, $\dot{P}$, spin-down luminosity, gamma-ray luminosity and galactic coordinates. The rotation period histograms are marginally different with 2.4σ pre-trial statistical significance. The post-trial

FIG. 6. Galactic coordinates of radio-loud and radio-quiet gamma-ray pulsars

FIG. 7. Distributions of galactic latitude b for radio-loud and radio-quiet pulsars. The two distrubutions are compatible with KS probability 99%
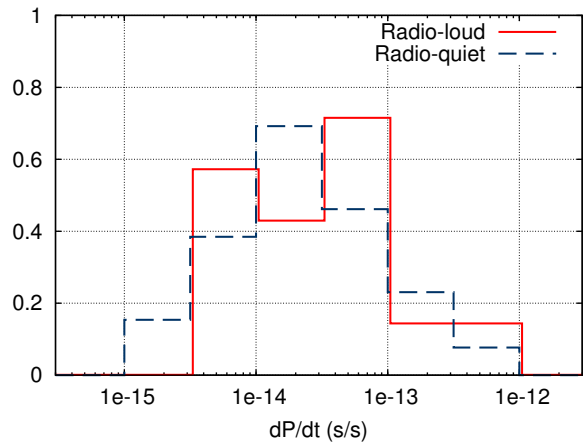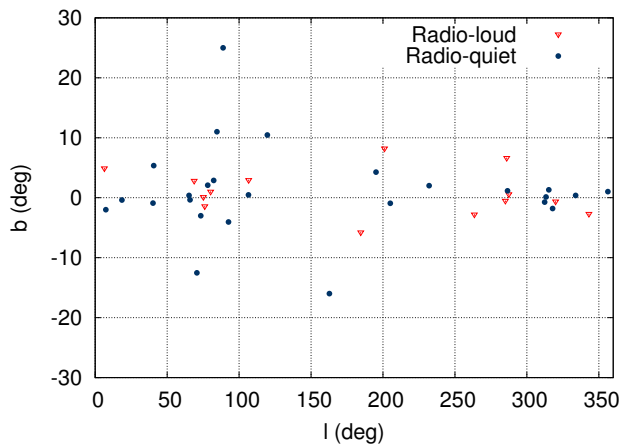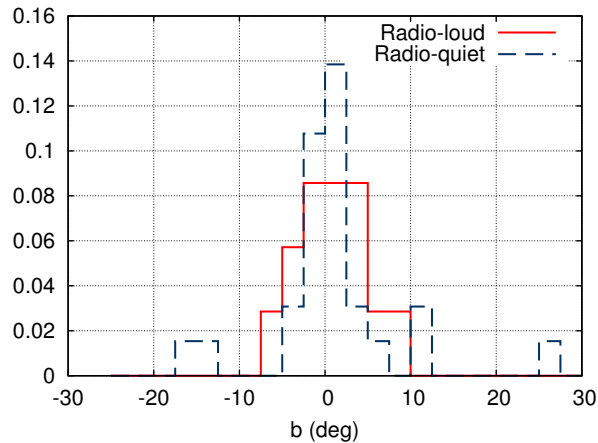
TABLE I. The KS-test probabilities for comparison of radio-quiet and radio-loud pulsar distributions over period, its time derivative, age, spin-down luminosity, energy flux above 100 MeV and galactic coordinates.

Parameter	KS probability
P $(1/f)$	1.5%
$\dot{P}$	85%
Age $(-f/2\dot{f})$	43%
Luminosity $(\sim f\dot{f})^{1/3}$	22%
Gamma energy flux	45%
l	87%
b	99%

significance is only 1.7σ taking into account that 6 independent tests are performed.

Based on the general agreement of the observed parameters of radio-loud and radio-quiet pulsars, one may assume that the chance probability of the particular pulsar to enter the blind search catalog do not depend on its radio emission properties. Therefore the fraction of the radio-quiet pulsars in the whole population of the gamma-ray pulsars may be estimated with the corresponding fraction in the catalog:

$$\epsilon_{RQ} = \frac{N_{RQ}}{N_{RQ} + N_{RL}} = 0.65 \pm 0.08\ (68\%CL), \quad (4)$$

where N_{RQ} and N_{RL} are numbers of radio-loud and radio-quiet non-recycled pulsars correspondingly. The result is in a good agreement with previous blind search [17].

Given that Fermi LAT observed 53 radio-loud pulsars and considering ϵ_{RQ} in its general sense, we predict that there are about 98 radio-quiet pulsars within the Fermi LAT sources for which the pulsations are detectable if the precise position and ephemerides are hypothetically known. Therefore, within these sources there are more than 60 radio-quiet pulsars with still undiscovered pulsed emission. These pulsars may be tracked when more gamma-ray data are available or with the future breakthrough blind search techniques.

Finally, let us compare our results with the published predictions of the emission models. The radio-quiet and radio-loud pulsar distribution with age are statistically compatible which contests the prediction of the PC models that the radio-quiet fraction depends on age. More specifically, the $\epsilon_{RQ}^{PC} \leq 0.53$ estimated for PC models and even smaller value at ages higher than 100 kyr [12] are in tension with our results. On the other hand, the $\epsilon_{RQ}^{OM} = 0.65$ estimated in the OM models [14] is in a perfect agreement with Eq. 4. While the catalog covers more than two thirds of the known radio-quiet pulsars, there is no indication of the evolution of the radio-beam solid angle proposed in [15].

Acknowledgments

[1] P. A. Caraveo, "Gamma-ray Pulsar Revolution," Annual Review of Astronomy and Astrophysics **52** (2014).

[2] I. A. Grenier and A. K. Harding, "Gamma-ray pulsars: a gold mine," Comptes Rendus Physique **16** (2015) 641.

[3] J. P. Halpern, S. S. Holt, "Discovery of soft X-ray pulsations from the gamma-ray source Geminga," Nature **357** (1992) 222-224.

[4] D. L. Bertsch, el al. "Pulsed high-energy gamma-radiation from Geminga (1E0630+178)" Nature **357** (1992) 306-307.

[5] A. A. Abdo, et al. " Detection of 16 Gamma-Ray Pulsars Through Blind Frequency Searches Using the Fermi LAT," Science **325** (2009) 840.

[6] P. M. Saz Parkinson, et al. "Eight gamma-ray Pulsars Discovered in Blind Frequency Searches of Fermi LAT Data," Astrophys. J., **725** (2010) 571-584.

[7] H. J. Pletsch, et al. "Discovery of Nine Gamma-Ray Pulsars in Fermi-LAT Data Using a New Blind Search

Method," Astrophys. J. **744** (2012) 105.

[8] H. J. Pletsch, et. al. "PSR J1838-0537: Discovery of a young, energetic gamma-ray pulsar" Astrophys. J., **755** (2012) L20.

[9] C. J. Clark *et al.*, Astrophys. J. **809** (2015) L2.

[10] P. A. Sturrock, "A Model of pulsars," Astrophys. J. **164** (1971) 529.

[11] S.J. Sturner, C.D. Dermer, "Statistics of γ-ray pulsars." A&AS **120** (1996) 99.

[12] P.L. Gonthier, M.S. Ouellette, J. Berrier, S. O'Brien, and A. K. Harding, "Galactic populations of radio and gamma-ray pulsars in the polar cap model," Astrophys. J. **565** (2002) 482.

[13] K. S. Cheng, C. Ho and M. A. Ruderman, "Energetic Radiation from Rapidly Spinning Pulsars. 1. Outer Magnetosphere Gaps. 2. Vela and Crab," Astrophys. J. **300** (1986) 500.

[14] B. B. P. Perera, M. A. McLaughlin, J. M. Cordes, M. Kerr, T. H. Burnett and A. K. Harding, "Modeling the non-recycled Fermi gamma-ray pulsar population," Astrophys. J. **776** (2013) 61.

[15] V. Ravi, R. N. Manchester and G. Hobbs, "Wide radio beams from gamma-ray pulsars," Astrophys. J., **716** (2010) L85-L89.

[16] K. P. Watters and R. W. Romani, Astrophys. J. **727** (2011) 123.

[17] G. I. Rubtsov and E. V. Sokolova, "Blind search for radio-quiet and radio-loud gamma-ray pulsars with Fermi-LAT data," JETP Lett. **100** (2015) 689.

[18] W. B. Atwood *et al.* [LAT Collaboration], "The Large Area Telescope on the Fermi Gamma-ray Space Telescope Mission," Astrophys. J. **697** (2009) 1071.

[19] http://fermi.gsfc.nasa.gov/ssc/data/access/

[20] F. Acero *et al.* [Fermi-LAT Collaboration], "Fermi Large Area Telescope Third Source Catalog," Astrophys. J. Suppl. **218** (2015) 23.

[21] http://www.fftw.org

[22] O.C. de Jager, B.C. Raubenheimer, J.W.H. Swanepoel, "A poweful test for weak periodic signals with unknown light curve shape in sparse data," A&A **221** (1989) 180.

[23] D. A. Kniffen, R. C. Hartman, D. J. Thompson, G. F. Bignami, C. E. Fichtel, T. Tumer, H. gelman, "Gamma radiation from the Crab Nebula above 35 MeV," Nature **251**, (1974) 397-399.

[24] Y. Ma, T. Lu, K. N. Yu, C. M. Young "Possible discovery of three gamma-ray pulsars," Astrophysics and Space Science **201** (1993) 113.

[25] P. M. Saz Parkinson "Status and Prospects of Fermi LAT Pulsar Blind Searches," AIP Conference Proceedings of Pulsar Conference 2010 "Radio Pulsars: a key to unlock the secrets of the Universe", Sardinia, October 2010

[26] D. J. Thompson, et al. Astrophys. J. **200** (1975) L79

[27] A. A. Abdo *et al.* [Fermi-LAT Collaboration], "Discovery of Pulsed Gamma Rays from the Young Radio Pulsar PSR J1028-5819 with the Fermi Large Area Telescope," Astrophys. J. **695** (2009) L72.

[28] D. J. Thompson "Gamma ray astrophysics: the EGRET results," Rep. Prog. Phys., **71** (2008) 116901

[29] P. Weltevrede *et al.* [Fermi-LAT Collaboration], "Gamma-ray and Radio Properties of Six Pulsars Detected by the Fermi Large Area Telescope" Astrophys. J. **708** (2010) 1426.

[30] D. J. Thompson, et al. "EGRET Observations of High-Energy Gamma Radiation from PSR B1706-44," Astrophys. J., **465** (1996) 385.

[31] P. V. Ramanamurthy et al. "EGRET detection of pulsed gamma radiation from PSR B1951+32," Astrophys. J., **447** (1995) L109.

[32] J. P. Halpern, et al. "Discovery of High-Energy Gamma-Ray Pulsations from PSR J2021+3651 with AGILE" Astrophys. J., **688** (2008) L33.

[33] F. Camilo, "PSR J2030+3641: Radio Discovery and Gamma-Ray Study of a Middle-aged Pulsar in the Now Identified Fermi-LAT Source 1FGL J2030.0+3641" Astrophys. J., **746** (2012) 39.

[34] J. P. Halpern, F. Camilo, E. V. Gotthelf, D. J. Helfand, M. Kramer, A. G. Lyne, K. M. Leighly & M. Eracleous, 2001a. "PSR J2229+6114: Discovery of an Energetic Young Pulsar in the Error Box of the EGRET Source 3EG J2227+6122," Astrophys. J., **552** (2001a) L125-L128

TABLE II. A catalog of gamma-ray pulsars found in a blind search. Frequency f and spin-down rate $\dot{f}$ of gamma pulsations correspond to the epoch MJD 55225. Characteristic age is estimated as $-f/2\dot{f}$. The last six columns contain the object information from the literature: pulsar name, J2000 galactic coordinates, Fermi LAT energy flux for $E > 100\,\mathrm{MeV}$ [20], type (Q - radio-quiet, L - radio-loud) and a reference to the first identification of gamma pulsations. New pulsars with respect to the catalog of the previous work [17] marked with an asterisk.

	Blind search results					Information from the literature					
no	3FGL name	H-test	f, Hz	$\dot{f}, -10^{-13}$ Hz s^{-1}	age, kyr	Pulsar name	l, deg	b, deg	G, 10^{-11} erg cm^{-2} s^{-1}	Type	Ref.
1	J0007.0+7302*	658	3.16574810	36.1543	14	PSR J0007+7303	119.66	10.46	42.6	Q	[5]
2	J0357.9+3206	485	2.25189503	0.6439	554	PSR J0357+3205	162.76	-15.99	6.6	Q	[5]
3	J0534.5+2201*	347	29.72749664	3716.0931	1.3	Crab pulsar	184.55	-5.78	147.2	L	[23]
4	J0633.7+0632	866	3.36250736	8.9973	59	PSR J0633+0632	205.10	-0.93	12.4	Q	[5]
5	J0633.9+1746	11253	4.21755990	1.9518	342	Geminga pulsar	195.13	4.27	415.3	Q	[3, 4]
6	J0659.5+1414	199	2.59796057	3.7094	111	Monogem pulsar	201.08	8.22	2.8	L	[24]
7	J0734.7-1558*	189	6.44573114	5.1970	197	PSR J0734-1559	232.05	2.01	4.2	Q	[25]
8	J0835.3-4510*	1353	11.18978060	156.0544	11	Vela pulsar	263.55	-2.79	893.0	L	[26]
9	J1028.4-5819	699	10.94042199	19.2705	90	PSR J1028-5819	285.07	-0.50	25.1	L	[27]
10	J1044.5-5737	252	7.19264583	28.2328	40	PSR J1044-5737	286.57	1.15	13.6	Q	[6]
11	J1048.2-5832	147	8.08368205	62.7274	20	PSR J1048-5832	287.43	0.58	20.1	L	[28]
12	J1057.9-5227	7561	5.07321957	1.5029	535	PSR J1057-5226	285.99	6.64	29.0	L	[28]
13	J1413.4-6205	371	9.11230510	22.9610	63	PSR J1413-6205	312.37	-0.73	19.8	Q	[6]
14	J1418.6-6058*	111	9.04346192	138.3125	10	PSR J1418-6058	313.32	0.13	31.0	Q	[5]
15	J1429.8-5910*	101	8.63231846	22.7099	60	PSR J1429-5911	315.26	1.32	8.8	Q	[6]
16	J1459.4-6053	313	9.69450009	23.7476	65	PSR J1459-6053	317.88	-1.80	11.0	Q	[5]
17	J1509.4-5850*	562	11.24546441	11.5913	154	PSR J1509-5850	319.98	-0.62	10.3	L	[29]
18	J1620.8-4928*	211	5.81616340	3.5480	260	PSR J1620-4927	333.90	0.39	18.0	Q	[7]
19	J1709.7-4429	3543	9.75607885	88.5318	17	PSR J1709-4429	343.10	-2.69	131.5	L	[30]
20	J1732.5-3130	1247	5.08792277	7.2603	111	PSR J1732-3131	356.31	1.02	14.9	Q	[5]
21	J1741.9-2054	5503	2.41720733	0.9926	386	PSR J1741-2054	6.41	4.90	11.8	L	[5]
22	J1809.8-2332	2790	6.81248050	15.9679	68	PSR J1809-2332	7.39	-2.00	44.8	Q	[5]
23	J1826.1-1256*	411	9.07223648	100.0361	14	PSR J1826-1256	18.56	-0.38	41.5	Q	[5]
24	J1836.2+5925	756	5.77154961	0.5005	1828	PSR J1836+5925	88.88	25.00	59.8	Q	[5]
25	J1846.3+0919	282	4.43357094	1.9521	360	PSR J1846+0919	40.69	5.35	2.5	Q	[6]
26	J1907.9+0602	210	9.37783521	76.9151	19	PSR J1907+0602	40.19	-0.90	31.9	Q	[5]
27	J1952.9+3253*	122	25.29478173	37.4774	107	PSR J1952+3252	68.78	2.83	15.1	L	[31]
28	J1954.2+2836*	127	10.78634243	24.6212	69	PSR J1954+2836	65.24	0.38	10.8	Q	[6]
29	J1957.7+5034	349	2.66804343	0.5043	839	PSR J1957+5033	84.60	11.01	3.2	Q	[6]
30	J1958.6+2845	452	3.44356138	25.1308	22	PSR J1958+2846	65.88	-0.35	9.9	Q	[5]
31	J2021.1+3651	562	9.63902020	89.0385	17	PSR J2021+3651	75.23	0.11	50.4	L	[32]
32	J2021.5+4026*	122	3.76904980	8.1591	73	PSR J2021+4026	78.23	2.08	88.3	Q	[5]
33	J2028.3+3332	323	5.65907212	1.5557	576	PSR J2028+3332	73.37	-3.00	6.4	Q	[7]
34	J2030.0+3642	192	4.99678975	1.6231	488	PSR J2030+3641	76.13	-1.43	4.6	L	[33]
35	J2030.8+4416*	160	4.40392491	1.2603	554	PSR J2030+4415	82.35	2.89	5.2	Q	[7]
36	J2032.2+4126	106	6.98089488	9.9452	111	PSR J2032+4127	80.22	1.02	16.0	L	[5]
37	J2055.8+2539	807	3.12928985	0.4016	1236	PSR J2055+2539	70.69	-12.53	5.5	Q	[6]
38	J2140.0+4715*	121	3.53545109	0.2225	2520	PSR J2139+4716	92.64	-4.04	2.3	Q	[7]
39	J2229.0+6114*	152	19.36285105	294.8890	10	PSR J2229+6114	106.65	2.95	23.5	L	[34]
40	J2238.4+5903	152	6.14486843	36.5838	27	PSR J2238+5903	106.55	0.48	5.9	Q	[5]